

Communications-Caching-Computing Tradeoff Analysis for Bidirectional Data Computation in Mobile Edge Networks

Yaping Sun, Lyutianyang Zhang, Zhiyong Chen, and Sumit Roy, *Fellow, IEEE*

Abstract—With the advent of the modern mobile traffic, e.g., online gaming, augmented reality delivery and etc., a novel bidirectional computation task model where the input data of each task consists of two parts, one generated at the mobile device in real-time and the other originated from the Internet proactively, is emerging as an important use case of 5G. In this paper, for ease of analytical analysis, we consider the homogeneous bidirectional computation task model in a mobile edge network which consists of one mobile edge computing (MEC) server and one mobile device, both enabled with computing and caching capabilities. Each task can be served via three mechanisms, i.e., local computing with local caching, local computing without local caching and computing at the MEC server. To minimize the average bandwidth, we formulate the joint caching and computing optimization problem under the latency, cache size and average power constraints. We derive the closed-form expressions for the optimal policy and the minimum bandwidth. The tradeoff among communications, computing and caching is illustrated both analytically and numerically, which provides insightful guideline for the network designers.

I. INTRODUCTION

The advent of modern mobile traffic, e.g., online gaming, mobile virtual reality (VR)/augmented reality (AR) delivery and etc., incurs ultra-high requirements on the wireless bandwidth [1]. For example, the mobile VR delivery requires the transmission rate on the order of G bit/s [2]. Mobile edge network (MEN) that equips the edge nodes of the mobile network, e.g., the mobile edge computing (MEC) server and the mobile devices, with caching and computing resources is deemed as one of the most promising approaches to alleviate the bandwidth burden on the mobile carriers [3]. In particular, mobile

edge caching indicates proactively storing popular contents into the network edge nodes to reduce the traffic redundancy and transmission latency [4], [5]. MEC refers to computing the tasks at the network edge nodes to reduce the core network burden and the latency [6]–[12]. How to efficiently utilize the caching and computing resources in MEN triggers the research interests from both the academic and industrial areas [9]–[15].

The computation model in the currently existing literature on MEC can be named as *one-way* computation task model. That is, the input data of each computation task is assumed to be either generated at the mobile device [9]–[11] or originated from the Internet [13]–[15]. In particular, in [9]–[11], the mobile device offloads the input data to the MEC server for computation and then downloads the output data from the MEC server. In [13]–[15], when the task is computed at the mobile device, the mobile device has to download the input data from the MEC server first if not cached locally and then computes the input data to obtain the output data.

Novelly, in this paper, we consider a *bidirectional* computation task model, where the input data consists of two parts, one of which is generated from the mobile device in real-time and the other of which is originated from the Internet proactively. One of the most directly motivating examples is online Role-Playing Game (RPG). Suppose one player is controlling a role and choosing which place/map to go. The location of the role combined with the map information from the MEC server could help render the picture for the player after some computations. The input data consists of these generated at the mobile device in real-time including current player equipment/weapon selection, strategy selection as well as role selection, and also those proactively generated from the Internet such as the map information. This rendering task could be done either at the mobile device or at the MEC server. If the task is computed at the MEC server, the mobile device has to first upload the player’s related information to the MEC server, then the MEC server computes the task and transmits the computation result to the mobile device. If

Yaping Sun and Zhiyong Chen are with Cooperative Medinet Innovation Center, Shanghai Jiao Tong University, Shanghai 200240, China (e-mail: {yapingsun, zhiyong.chen}@sjtu.edu.cn). Lyutianyang Zhang and Sumit Roy are with Department of Electrical & Computer Engineering, University of Washington, Seattle, WA, USA (e-mail: {lyutiz, sroy}@uw.edu).

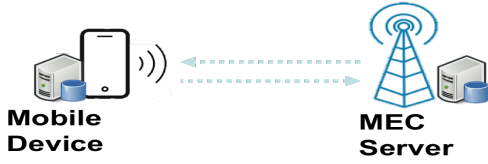


Fig. 1: System Model

the task is computed at the mobile device, the mobile device has to first download the map information from the MEC server and then computes the rendering task. Since the required transmission load and the computation frequency when computing at the mobile device are different from those when computing at the MEC server, the corresponding consumed bandwidth differs and thus the computing policy requires careful design. Besides, the history of all the players' actions could provide a popularity distribution of the map preferences, e.g., the maps/places the players mostly like to go to. Based on a priori knowledge of the popularity, the popular maps/places could be proactively cached at the mobile device to save the consumed bandwidth.

Inspired by this, under the latency, cache size and average power constraints, this paper jointly optimizes the computing and caching policy to minimize the average bandwidth for the bidirectional computation task model. Then, we derive the closed-form expressions for the optimal policy and the minimum bandwidth in the homogeneous scenario. The tradeoff among communications, computing and caching (3C) is at last illustrated both theoretically and numerically.

II. SYSTEM MODEL

As illustrated in Fig. 1, we consider a mobile edge network consisting of one MEC server and one mobile device, both equipped with certain caching and computing abilities. The mobile device is assumed to request one task at each time.

A. Task Model

Assume that there are F tasks in total to be requested by the mobile device. Denote with $\mathcal{F} \triangleq \{1, 2, \dots, f, \dots, F\}$ the task set. Each task $f \in \mathcal{F}$ is characterized by a 5-item tuple $\{I^D$ (in bits), I^S (in bits), O (in bits), w (in cycles/bit), τ (in seconds) $\}^1$. In particular, for each task $f \in \mathcal{F}$, I^D represents the size of the local input data which is

generated at the mobile device in real time. I^S represents the size of the remote input data which is originated from the Internet and can be proactively stored. O represents the size of the output data. w and τ denote the required computation cycles per bit and the maximum tolerable service latency, respectively. Since the input remote data is generated proactively, the task popularity can be learned based on the request history information. The task request process at the mobile device is assumed to conform to the independent reference model based on the following assumptions [14]: i) the tasks that the mobile device wants to process is fixed to the set \mathcal{F} ; ii) each probability of task f to be requested, denoted as P_f , is assumed to be independent identical distributed (i.i.d.). Namely, $\sum_{f=1}^F P_f = 1$. In particular, we consider a homogeneous scenario, i.e., $P_f = \frac{1}{F}$. Since the local input data is generated in real time, its content may vary from time to time. However, the input local data size is assumed to be unchanged.

B. Caching and Computing Model

First, consider the cache placement at the mobile device. From the above-mentioned task model, we can see that only caching of the remote input data can be considered. Denote with $c_f \in \{0, 1\}$ the caching decision of task $f \in \mathcal{F}$, where $c_f = 1$ means that the remote input data is cached at the mobile device and $c_f = 0$, otherwise. Denote with C (in bits) the cache size at the mobile device and the caching constraint is given by

$$\sum_f I^S c_f \leq C. \quad (1)$$

All the remote input data are assumed to be proactively cached at the MEC server considering the storage size at the MEC server is generally large enough.

Next, consider the computing decision at the mobile device. Denote with $d_f \in \{0, 1\}$ the computing decision of task $f \in \mathcal{F}$, where $d_f = 1$ means that task f is computed at the mobile device and $d_f = 0$ means that task f is computed at the MEC server. Denote with f_D (in cycles/second) the computation frequency of the mobile device and f_S (in cycles/second) the computation frequency of the MEC server. The energy consumed for computing one cycle with frequency f_D at the mobile device is μf_D^2 , where μ is the effective switched capacitance related to the chip architecture and can indicate the power efficiency of CPU at the mobile device [16]. Denote with \bar{P} (in W) the average available power at the mobile device. We assume that there is no power constraint at the MEC server considering the MEC server is in general connected to a power grid.

¹This system model can be directly extended to a multi-user heterogeneous scenario.

C. Service Mechanism

Based on the joint caching and computing decision ($\mathbf{c} \triangleq (c_f)_{f \in \mathcal{F}}$, $\mathbf{d} \triangleq (d_f)_{f \in \mathcal{F}}$), each task $f \in \mathcal{F}$ can be served via the following three routes.

- **Local computing with local caching.** When $d_f = 1$ and $c_f = 1$, the mobile device immediately computes task f based on the real-time local input data and the locally cached remote input data. The required latency is the computation latency at the mobile device only, i.e., $\frac{(I^S + I^D)w}{f_D} d_f$. For satisfying the latency constraint, we assume that $\frac{(I^S + I^D)w}{f_D} \leq \tau$. The average consumed power at the mobile device for task f is the consumed computation power only, i.e., $\frac{\mu f_D^2 w (I^D + I^S)}{F\tau} d_f$.
- **Local computing without local caching.** When $d_f = 1$ and $c_f = 0$, the mobile device first downloads the remote input data from the MEC server and then computes the task locally. The required latency includes the downloading latency and the local computation latency, i.e.,

$$\left(\frac{I^S}{B_f^D \log(1 + \frac{P_D h^2}{N_0})} + \frac{(I^S + I^D)w}{f_D} \right) d_f (1 - c_f) \leq \tau, \quad (2)$$

where B_f^D is the downlink bandwidth allocated for the transmission of task f , P_D is the average downlink power spectrum density (PSD) at the MEC server, h is the channel coefficient and N_0 is the average PSD of the channel noise. The average consumed power at the mobile device for task f is the consumed computation power only, $\frac{\mu f_D^2 w (I^D + I^S)}{F\tau} d_f$.

- **MEC computing.** When $d_f = 0$, the mobile device first uploads the local input data to the MEC server. After receiving the local input data, the MEC server computes task f and then transmits the output data to the mobile device. The required latency includes the uplink transmission latency, the computation latency at the MEC server, and the downlink transmission latency, i.e.,

$$\left(\frac{I^D}{B_f^U \log(1 + \frac{P_U h^2}{N_0})} + \frac{(I^S + I^D)w}{f_S} + \frac{O_f}{B_f^D \log(1 + \frac{P_D h^2}{N_0})} \right) (1 - d_f) \leq \tau, \quad (3)$$

where B_f^U is the uplink bandwidth allocated to the mobile device and P_U is the average uplink PSD at the mobile device. The average consumed power at the mobile device for task f is the average uplink transmission power, i.e., $\frac{P_U I^D}{F\tau \log(1 + \frac{P_U h^2}{N_0})} (1 - d_f)$.

From above, under the average power constraint at the mobile device, we have

$$\sum_{f=1}^F \left(\frac{\mu f_D^2 w (I^D + I^S)}{F\tau} d_f + \frac{P_U I^D}{F\tau \log(1 + \frac{P_U h^2}{N_0})} (1 - d_f) \right) \leq \bar{P}. \quad (4)$$

The average consumed bandwidth, including both uplink and downlink bandwidth, is given by

$$\frac{1}{F} \sum_{f=1}^F (B_f^U + B_f^D). \quad (5)$$

III. PROBLEM FORMULATION AND OPTIMAL PROPERTY ANALYSIS

A. Problem Formulation

We formulate the joint caching and computing optimization problem to minimize the average required bandwidth, including both the uplink and downlink bandwidth, subject to the cache size, average power and latency constraints, as below.

Problem 1 (Joint Caching and Computing Optimization).

$$\begin{aligned} \min_{\mathbf{c}, \mathbf{d}} \quad & \frac{1}{F} \sum_{f=1}^F (B_f^U + B_f^D) \\ \text{s.t.} \quad & (1), (2), (3), (4), \\ & c_f \in \{0, 1\}, d_f \in \{0, 1\}, f \in \mathcal{F}. \end{aligned}$$

Denote with ($\mathbf{c}^* \triangleq (c_f^*)_{f \in \mathcal{F}}$, $\mathbf{d}^* \triangleq (d_f^*)_{f \in \mathcal{F}}$) the optimal joint caching and computing policy and B^* the corresponding optimal average bandwidth.

B. Optimal Properties

First, we can directly observe the following property between the local computing and local caching.

Property 1. When $d_f = 0$, $c_f = 0$ without loss of optimality.

Then, for each $f \in \mathcal{F}$, introduce $x_{f,j} \in \{0, 1\}$, $j \in \{1, 2, 3\}$, with $x_{f,j} = 1$ indicating that task f is served via the j -th route and $x_{f,j} = 0$ otherwise. Here, the first route corresponds to the local computing with local caching, i.e., $d_f = 1$, $c_f = 1$. The second refers to the local computing without caching, i.e., $d_f = 1$, $c_f = 0$. The third refers to the MEC computing, i.e., $d_f = 0$, $c_f = 0$. Denote with $B_{f,j}$, $j \in \{1, 2, 3\}$ the minimum value of $B_f^U + B_f^D$ for the j -th route given (\mathbf{c} , \mathbf{d}).

Next, under latency constraint, we obtain the analytical expression for $B_{f,j}$.

Property 2. When $d_f = 1$, $c_f = 1$, i.e., $x_{f,1} = 1$, $B_{f,1} = 0$.

Property 3. When $d_f = 1$, $c_f = 0$, i.e., $x_{f,2} = 1$, $B_{f,2} = \frac{I^S}{\left(\tau - \frac{(I^S + I^D)w}{f_D}\right) \log\left(1 + \frac{P_D h^2}{N_0}\right)}$.

Property 3 can be obtained directly from (2).

Property 4. When $d_f = 0$, $c_f = 0$, i.e., $x_{f,3} = 1$, $B_{f,3} = \frac{(\sqrt{a_1} + \sqrt{a_2})^2}{a_3}$, where $a_1 = \frac{I^D}{\log\left(1 + \frac{P_U h^2}{N_0}\right)}$, $a_2 = \frac{O}{\log\left(1 + \frac{P_D h^2}{N_0}\right)}$, and $a_3 = \tau - \frac{(I^S + I^D)w}{f_S}$.

Proof. Proof of Property 4 can be seen in Appendix A. \square

After that, via replacing $B_f^U + B_f^D$ in the objective function of Problem 1 with $B_{f,j}$ obtained from Properties 2-4, the latency constraints (2) and (3) can be eliminated. Denote with $X_j \triangleq \sum_{f=1}^F x_{f,j}$, $j \in \{1, 2, 3\}$ the number of tasks served via the j -th route. Since each task is independent of each other and homogeneous, given $(X_j)_{j \in \{1, 2, 3\}}$, $(x_{f,j})_{f \in \mathcal{F}, j \in \{1, 2, 3\}}$ can be obtained via

$$x_{f,1} = \begin{cases} 1 & i = 1, \dots, X_1, \\ 0 & \text{otherwise,} \end{cases} \quad (6)$$

$$x_{f,2} = \begin{cases} 1 & i = X_1 + 1, \dots, X_1 + X_2, \\ 0 & \text{otherwise,} \end{cases} \quad (7)$$

$$x_{f,3} = \begin{cases} 1 & i = X_1 + X_2 + 1, \dots, X_1 + X_2 + X_3, \\ 0 & \text{otherwise.} \end{cases} \quad (8)$$

Via replacing $(x_{f,j})_{f \in \mathcal{F}, j \in \{1, 2, 3\}}$ with $(X_j)_{j \in \{1, 2, 3\}}$, Problem 1 is transformed into Problem 2 equivalently.

Problem 2 (Equivalent Optimization).

$$\min_{(X_j)_{j \in \{1, 2, 3\}}} X_1 B_1 + X_2 B_2 + X_3 B_3 \quad (9)$$

$$s.t. \quad I^S X_1 \leq C, \quad (10)$$

$$k_1(X_1 + X_2) + k_2 X_3 \leq \bar{P}, \quad (11)$$

$$X_1 + X_2 + X_3 = F, \quad (12)$$

$$0 \leq X_1 \leq F, \quad (13)$$

$$0 \leq X_2 \leq F, \quad (14)$$

$$0 \leq X_3 \leq F, \quad (15)$$

where $k_1 \triangleq \frac{\mu f_D^2 w (I^D + I^S)}{\tau F}$ and $k_2 \triangleq \frac{P_U I^D}{F \tau \log\left(1 + \frac{P_U h^2}{N_0}\right)}$ represent the average power consumed at the mobile

device of each task for local computing and uplink transmission, respectively.

IV. OPTIMAL POLICY AND TRADEOFF ANALYSIS

A. Optimal Policy

Theorem 1. (Optimal joint policy when $k_1 > k_2$) If $B_3 > B_2$, the optimal joint policy is given as

$$\begin{aligned} X_1 &= \min \left\{ \left\lfloor \frac{C}{I^S} \right\rfloor, F, \left\lfloor \frac{\bar{P} - F k_2}{k_1 - k_2} \right\rfloor \right\}, \\ X_2 &= \max \left\{ 0, \min \left\{ F, \left\lfloor \frac{\bar{P} - F k_2}{k_1 - k_2} \right\rfloor \right\} - X_1 \right\}, \\ X_3 &= F - X_1 - X_2, \end{aligned} \quad (16)$$

where $\lfloor \bullet \rfloor$ denotes the round-down function. $B^* = B_2 X_2 + B_3 X_3$. If $B_3 \leq B_2$, the optimal joint policy is given as

$$\begin{aligned} X_1 &= \min \left\{ \left\lfloor \frac{C}{I^S} \right\rfloor, F, \left\lfloor \frac{\bar{P} - F k_2}{k_1 - k_2} \right\rfloor \right\}, \\ X_2 &= 0, \\ X_3 &= F - X_1. \end{aligned} \quad (17)$$

$B^* = B_3 X_3$.

Proof. Proof of Theorem 1 can be seen in Appendix B. \square

Theorem 2. (Optimal joint policy when $k_1 \leq k_2$) If $B_3 > B_2$, the optimal joint policy is given as

$$\begin{aligned} X_1 &= \left\lfloor \frac{C}{I^S} \right\rfloor, \\ X_2 &= F - X_1, \\ X_3 &= 0. \end{aligned} \quad (18)$$

$B^* = B_2 X_2$. If $B_3 \leq B_2$, the optimal joint policy is

$$\begin{aligned} X_1 &= \left\lfloor \frac{C}{I^S} \right\rfloor, \\ X_2 &= \max \left\{ 0, \left\lfloor \frac{\bar{P} - F k_2}{k_2 - k_1} \right\rfloor - X_1 \right\}, \\ X_3 &= F - X_1 - X_2. \end{aligned} \quad (19)$$

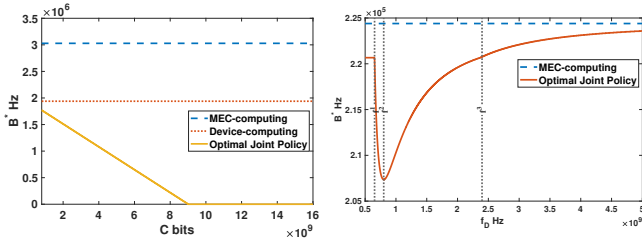
$B^* = B_2 X_2 + B_3 X_3$.

Proof. Proof of Theorem 2 can be seen in Appendix C. \square

B. Tradeoff Analysis

1) $k_1 > k_2$: When $k_1 > k_2$ and $B_3 > B_2$, from (16), there are three possible cases as below.

- When $\left\lfloor \frac{\bar{P} - F k_2}{k_1 - k_2} \right\rfloor < \left\lfloor \frac{C}{I^S} \right\rfloor < F$, $X_1 = \left\lfloor \frac{\bar{P} - F k_2}{k_1 - k_2} \right\rfloor$ decreases with f_D since k_1 increases with f_D , $X_2 =$



(a) Cache size when $f_D = 4$ GHz and $\tau = 0.5$ s. (b) Computing frequency when $C = 400$ MB and $\tau = 0.143$ s.

Fig. 2: Impact of C and f_D on B^* . $f_S = 15$ GHz, $F = 300$, $\frac{P_D h^2}{N_0} = 28.1573$ dB, $\frac{P_U h^2}{N_0} = 10.98$ dB, $P_U = \frac{250}{180}$ mW/KHz, $P_D = \frac{5}{180}$ W/KHz, $w = 10$, $\mu = 10^{-27}$.

0 is independent of f_D and $X_3 = F - X_1$ increases with f_D . Then, $B^* = B_3 X_3$ increases with f_D with B_3 given in Property 4 independent of f_D . This is because when the locally available power is limited, increasing f_D decreases the number of tasks that can be computed locally. Also, B^* is independent of C indicating that it is mainly limited by the local computing power $\left\lfloor \frac{\bar{P} - Fk_2}{k_1 - k_2} \right\rfloor$.

- When $\left\lfloor \frac{C}{I^S} \right\rfloor < \left\lfloor \frac{\bar{P} - Fk_2}{k_1 - k_2} \right\rfloor < F$, $X_1 = \left\lfloor \frac{C}{I^S} \right\rfloor$ is independent of f_D , $X_2 = \left\lfloor \frac{\bar{P} - Fk_2}{k_1 - k_2} \right\rfloor - X_1$ decreases with f_D since k_1 increases with f_D , and X_3 increases with f_D . Then, B^* increases with f_D since $B_2 < B_3$. Meanwhile, B^* decreases with C .
- When $\left\lfloor \frac{C}{I^S} \right\rfloor < F < \left\lfloor \frac{\bar{P} - Fk_2}{k_1 - k_2} \right\rfloor$, $X_1 = \left\lfloor \frac{C}{I^S} \right\rfloor$ and $X_2 = F - X_1$ are independent of f_D and $X_3 = 0$ is independent of f_D . Then, since B_2 given in Property 3 decreases with f_D , $B^* = B_2 X_2$ decreases with f_D . This is because when the locally available power is large enough, increasing f_D decreases the computation latency. Also, B^* decreases with C .

When $k_1 > k_2$ and $B_3 \leq B_2$, from (17), there are three possible cases as below.

- When $\left\lfloor \frac{\bar{P} - Fk_2}{k_1 - k_2} \right\rfloor < \left\lfloor \frac{C}{I^S} \right\rfloor < F$, $X_1 = \left\lfloor \frac{\bar{P} - Fk_2}{k_1 - k_2} \right\rfloor$ decreases with f_D , $X_2 = 0$ is independent of f_D and $X_3 = F - X_1$ increases with f_D . Then, $B^* = B_3 X_3$ is independent of C and increases with f_D . This is because when the locally available power is limited, i.e., smaller than the number of tasks that can be cached locally $\frac{C}{I^S}$, increasing f_D decreases the number of tasks that can be computed locally.
- When $\left\lfloor \frac{C}{I^S} \right\rfloor < \left\lfloor \frac{\bar{P} - Fk_2}{k_1 - k_2} \right\rfloor < F$, $X_1 = \left\lfloor \frac{C}{I^S} \right\rfloor$, $X_2 = 0$ and $X_3 = F - X_1$ which are all independent of f_D . Then, we have $B^* = B_3 X_3$ independent of f_D and decreases with C . This is because when $\left\lfloor \frac{C}{I^S} \right\rfloor <$

$\left\lfloor \frac{\bar{P} - Fk_2}{k_1 - k_2} \right\rfloor < F$, the bandwidth gain is limited by the local cache size C .

- When $\left\lfloor \frac{C}{I^S} \right\rfloor < F < \left\lfloor \frac{\bar{P} - Fk_2}{k_1 - k_2} \right\rfloor$, $X_1 = \left\lfloor \frac{C}{I^S} \right\rfloor$, $X_2 = 0$ and $X_3 = F - X_1$ are independent of f_D . Then, B^* is independent of f_D and decreases with C .

From Fig. 2 (a), we can see that joint caching and computing at the mobile device helps further reduce the bandwidth compared with computing only either at the MEC server or at the mobile device. From Fig. 2 (b), firstly, when f_D is relatively small, $B_2 \geq B_3$, $k_1 > k_2$ and $\left\lfloor \frac{C}{I^S} \right\rfloor < F < \left\lfloor \frac{\bar{P} - Fk_2}{k_1 - k_2} \right\rfloor$, and thus bandwidth remains unchanged with f_D . The first turning point f^1 appears when $B_3 = B_2$. By setting $B_3 = B_2$, the switching point f^1 could be explicitly expressed as

$$f^1 = \frac{(I^S + I^D)w}{\tau - \frac{a_3 I^S}{\log(1 + \frac{P_D h^2}{N_0})(\sqrt{a_1} + \sqrt{a_2})^2}}. \quad (20)$$

Then, the bandwidth starts decreasing with f_D . This is because as f_D increases, $B_2 < B_3$, $k_1 > k_2$ and $\left\lfloor \frac{C}{I^S} \right\rfloor < F < \left\lfloor \frac{\bar{P} - Fk_2}{k_1 - k_2} \right\rfloor$. Then, the second turning point f^2 appears when $\left\lfloor \frac{\bar{P} - Fk_2}{k_1 - k_2} \right\rfloor = F$. By setting $\left\lfloor \frac{\bar{P} - Fk_2}{k_1 - k_2} \right\rfloor = F$, we could obtain the explicit expression for the second turning point

$$f^2 \approx \sqrt{\frac{\tau(\bar{P} - Fk_2) + \tau Fk_2}{\mu w(I^D + I^S)}}. \quad (21)$$

Next, the bandwidth B^* starts increasing with f_D . This is because as f_D increases, $\left\lfloor \frac{C}{I^S} \right\rfloor < \left\lfloor \frac{\bar{P} - Fk_2}{k_1 - k_2} \right\rfloor < F$. Moreover, we could observe that there is another turning point which pushes the optimal policy towards the bandwidth of MEC-computing policy eventually. This turning point happens when $\left\lfloor \frac{C}{I^S} \right\rfloor = \left\lfloor \frac{\bar{P} - Fk_2}{k_1 - k_2} \right\rfloor$. By setting $\left\lfloor \frac{C}{I^S} \right\rfloor = \left\lfloor \frac{\bar{P} - Fk_2}{k_1 - k_2} \right\rfloor$, the turning point f^3 can be expressed as

$$f^3 \approx \sqrt{\frac{\tau F I^S (\bar{P} - Fk_2)}{\mu w (I^S + I^D) C} + \frac{\tau F k_2}{\mu w (I^S + I^D)}}. \quad (22)$$

When $f_D > f^3$, the optimal policy is the scenario where $k_1 > k_2$, $B_3 > B_2$ and $\left\lfloor \frac{\bar{P} - Fk_2}{k_1 - k_2} \right\rfloor < \left\lfloor \frac{C}{I^S} \right\rfloor < F$. The optimal policy converges to the MEC computing policy as f_D goes to infinity, i.e., $X_3 = F$.

2) $k_1 \leq k_2$: When $k_1 \leq k_2$ and $B_3 > B_2$, from (18), there is only one possible case. The bandwidth gain mainly comes from the local computing with/without caching. The MEC computing does not bring any gain.

V. CONCLUSION

In this paper, we consider a novel bidirectional computation task model and formulate the joint caching and computing optimization problem to minimize the average bandwidth under the latency, cache size and average power constraints. We derive the closed-form expressions for the optimal policy and the minimum bandwidth, which illustrates that the 3C tradeoff can be classified into nine regions according to the relationship between the cache and computation capabilities at the mobile device, that between the uplink transmission power consumption and the local computation power consumption.

APPENDIX A: PROOF OF PROPERTY 4

For each task $f \in \mathcal{F}$, when $d_f = 0$, we have $\frac{I_f^P}{B_f^U \log(1 + \frac{P_U h^2}{N_0})} + \frac{(I_f^S + I_f^P)w_f}{f_S} + \frac{O_f}{B_f^D \log(1 + \frac{P_D h^2}{N_0})} \leq \tau$. Hence, $B_{f,3}$ can be obtained via solving the following optimization problem:

$$\begin{aligned} \min_{B_f^U, B_f^D} \quad & B_f^U + B_f^D \\ \text{s.t.} \quad & \frac{a_1}{B_f^U} + \frac{a_2}{B_f^D} \leq a_3, \\ & B_f^U > 0, \\ & B_f^D > 0, \end{aligned} \quad (23)$$

where $a_1 = \frac{I_f^P}{\log(1 + \frac{P_U h^2}{N_0})} > 0$, $a_2 = \frac{(I_f^S + I_f^P)w_f}{f_0} > 0$ and $a_3 = \tau - \frac{O_f}{\log(1 + \frac{P_D h^2}{N_0})} > 0$. We can see that Problem 10 is a convex minimization problem. Denote with B_f^{U*} and B_f^{D*} the optimal solution to Problem 10. In order to solve Problem 10, let us first consider a modified version of the above convex problem as below.

$$\begin{aligned} \min_{B_f^U, B_f^D} \quad & B_f^U + B_f^D \\ \text{s.t.} \quad & \frac{a_1}{B_f^U} + \frac{a_2}{B_f^D} \leq a_3. \end{aligned} \quad (24)$$

If the solution to Problem 11 satisfies $B_f^{U*} > 0$ and $B_f^{D*} > 0$, then it is also a solution to Problem 10. Based on KKT conditions of Problem 11, we get an optimal solution to Problem 11 as below.

$$B_f^{U*} = \frac{a_1 + \sqrt{a_1 a_2}}{a_3} > 0 \quad (25)$$

$$B_f^{D*} = \frac{a_2 + \sqrt{a_1 a_2}}{a_3} > 0. \quad (26)$$

Therefore, we get B_f^{U*} and B_f^{D*} of Problem 10, and then $B_{f,3} = B_f^{U*} + B_f^{D*}$. The proof ends.

APPENDIX B: PROOF OF THEOREM 1

- Suppose $B_3 > B_2$ and $k_1 - k_2 > 0$, from Problem. (9) constraint (11), we could obtain an upper-bound, $X_1 + X_2 \leq \lfloor \frac{\bar{P} - Fk_2}{k_1 - k_2} \rfloor$. Meanwhile, constraint. (10) yields upper-bound $X_1 \leq \lfloor \frac{C}{I^S} \rfloor$. Since $B_1 = 0$, assigning as much files to processing method 1 as possible is the best policy. Meanwhile, X_1 cannot be larger than the total number of files F obviously. Therefore, we have $X_1 = \min\{\lfloor \frac{C}{I^S} \rfloor, F, \lfloor \frac{\bar{P} - Fk_2}{k_1 - k_2} \rfloor\}$. Subsequently, because $B_3 > B_2$, assigning files to processing method 2 is the optimal policy with the constraint of $X_1 + X_2 \leq \lfloor \frac{\bar{P} - Fk_2}{k_1 - k_2} \rfloor$ which could be larger than the total number of files. Hence, $X_2 = \max\{0, \min\{F, \lfloor \frac{\bar{P} - Fk_2}{k_1 - k_2} \rfloor\} - X_1\}$. Last but not least, $X_3 = F - X_1 - X_2$.
- If $B_3 \leq B_2$ and $k_1 - k_2 > 0$, from Problem. (9) constraint (11), we could obtain an upper-bound, $X_1 + X_2 \leq \lfloor \frac{\bar{P} - Fk_2}{k_1 - k_2} \rfloor$. Meanwhile, constraint (10) yields upper-bound $X_1 \leq \lfloor \frac{C}{I^S} \rfloor$. Since $B_1 = 0$, assigning as much files to processing method 1 as possible is the best policy. Therefore, similarly with the above proof, we have $X_1 = \min\{\lfloor \frac{C}{I^S} \rfloor, F, \lfloor \frac{\bar{P} - Fk_2}{k_1 - k_2} \rfloor\}$. Because $B_3 \leq B_2$, assigning files to processing method 3 is the optimal policy. So we do not utilize process method at all. Hence, $X_2 = 0$ and $X_3 = F - X_1$.

The proof ends here.

APPENDIX C: PROOF OF THEOREM 2

- Suppose $B_3 > B_2$ and $k_1 - k_2 \leq 0$. Constraint (11) yields that $X_1 + X_2 \geq \lceil \frac{\bar{P} - k_2 F}{k_1 - k_2} \rceil$. Meanwhile, constraint (10) yields $X_1 \leq \lfloor \frac{C}{I^S} \rfloor$. Therefore, we have only one upper-bound and we set $X_1 = \lfloor \frac{C}{I^S} \rfloor$. Since $B_3 > B_2$, we set $X_2 = F - X_1$ and $X_3 = 0$.
- Suppose $B_3 \leq B_2$ and $k_1 - k_2 \leq 0$. Similarly, one upper-bound indicates that $X_1 = \lfloor \frac{C}{I^S} \rfloor$. Since $B_3 \leq B_2$, we get rid of X_2 as much as possible by setting $X_2 = \max\{0, \lceil \frac{\bar{P} - Fk_2}{k_1 - k_2} \rceil - X_1\}$. Note that it is possible for $\frac{\bar{P} - k_2 F}{k_1 - k_2}$ to be negative so that there is no constraint for X , which means there is no constraint on X_2 and it could be zero directly. Last, $X_3 = F - X_1 - X_2$.

The proof ends here.

REFERENCES

- [1] J. Hecht, "The bandwidth bottleneck that is throttling the internet," *Nature News*, vol. 536, no. 7615, p. 139, Aug. 2016.

- [2] E. Bastug, M. Bennis, M. Médard, and M. Debbah, "Toward interconnected virtual reality: Opportunities, challenges, and enablers," *IEEE Communications Magazine*, vol. 55, no. 6, pp. 110–117, June 2017.
- [3] H. Liu, Z. Chen, and L. Qian, "The three primary colors of mobile systems," *IEEE Commun. Mag.*, vol. 54, no. 9, pp. 15–21, Sep. 2016.
- [4] M. A. Maddah-Ali and U. Niesen, "Fundamental limits of caching," *IEEE Transactions on Information Theory*, vol. 60, no. 5, pp. 2856–2867, May 2014.
- [5] Y. Sun, Y. Cui, and H. Liu, "Joint pushing and caching for bandwidth utilization maximization in wireless networks," *IEEE Transactions on Communications*, vol. 67, no. 1, pp. 391–404, Dec. 2018.
- [6] M. Patel, Y. Hu, P. Hede, J. Joubert, C. Thornton, B. Naughton, J. Roldan Ramos, C. Chan, V. Young, S. Jin Tan, D. Lynch, N. Sprecher, T. Musiol, C. Manzanares, U. Rauschenbach, S. Abeta, L. Chen, K. Shimizu, A. Neal, P. Cosimini, A. Pollard, and G. Klas, "Mobile edge computing-introductory technical white paper," *Mobile-Edge Computing (MEC) ISG, European Telecommunications Standards Institute (ETSI)*, Sep. 2014.
- [7] P. Mach and Z. Becvar, "Mobile edge computing: A survey on architecture and computation offloading," *IEEE Communications Surveys & Tutorials*, vol. 19, no. 3, pp. 1628–1656, Mar. 2017.
- [8] Y. Mao, C. You, J. Zhang, K. Huang, and K. B. Letaief, "A survey on mobile edge computing: The communication perspective," *IEEE Communications Surveys Tutorials*, vol. 19, no. 4, pp. 2322–2358, Aug. 2017.
- [9] C. You, K. Huang, H. Chae, and B. Kim, "Energy-efficient resource allocation for mobile-edge computation offloading," *IEEE Trans. Wireless Commun.*, vol. 16, no. 3, pp. 1397–1411, Mar. 2017.
- [10] Y. Mao, J. Zhang, and K. B. Letaief, "Dynamic computation offloading for mobile-edge computing with energy harvesting devices," *IEEE Journal on Selected Areas in Communications*, vol. 34, no. 12, pp. 3590–3605, Dec. 2016.
- [11] T. Q. Dinh, J. Tang, Q. D. La, and T. Q. S. Quek, "Offloading in mobile edge computing: Task allocation and computational frequency scaling," *IEEE Transactions on Communications*, vol. 65, no. 8, pp. 3571–3584, Aug. 2017.
- [12] L. Liu, C. Chen, Q. Pei, S. Maharjan, and Y. Zhang, "Vehicular edge computing and networking: A survey," *arXiv preprint arXiv:1908.06849*, 2019.
- [13] X. Yang, Z. Chen, K. Li, Y. Sun, N. Liu, W. Xie, and Y. Zhao, "Communication-constrained mobile edge computing systems for wireless virtual reality: Scheduling and tradeoff," *IEEE Access*, vol. 6, pp. 16665–16677, Mar. 2018.
- [14] Y. Sun, Z. Chen, M. Tao, and H. Liu, "Communications, caching, and computing for mobile virtual reality: Modeling and tradeoff," *IEEE Transactions on Communications*, vol. 67, no. 11, pp. 7573–7586, Nov. 2019.
- [15] —, "Bandwidth gain from mobile edge computing and caching in wireless multicast systems," *submitted to IEEE Trans. Wireless Commun.*, arxiv.org/abs/1901.09738, 2019.
- [16] Y. Mao, J. Zhang, S. Song, and K. B. Letaief, "Power-delay tradeoff in multi-user mobile-edge computing systems," in *2016 IEEE Global Communications Conference (GLOBECOM)*, Feb. 2016.